

# 10eV - 30 keV における固体中の電子阻止能の 計算

**H. Shinotsuka, S. Tanuma, C. J. Powell\*, and D. R. Penn\***

National Institute for Materials Science (NIMS)

\*National Institute of Standards and Technology (NIST)

1. Introduction
2. Calculation of SPs from optical data
  - Relativistic differential cross section (DCS)
  - SPs from full Penn algorithm (FPA )
  - Influence of electron exchange effect
3. Comparison of calculation models for SPs
  - Full Pen algorithm, Single pole approximation, Mermin-type ELF  
N-oscillator model, Relativistic Bethe equation
4. Comparison of SPs from experiments
5. Summary

# 1. Introduction

- : Electron Stopping Power (SP) is an important parameter in
- radiation dosimetry
  - modeling of electron transport in matter for many applications.
- SP has been used in Monte Carlo simulations of electron transport : EPMA, AES, dimensional metrology in SEM, etc ....

## The SP values

- Bethe equation (valid only above 10 keV!)
- Energies  $< 2$  keV are very important for surface analysis
- In previous, we calculated them from optical ELF using single pole approximation (SPA) over 100 eV to 30 keV.

We extended the SP calculations down to 10 eV ( 10 eV – 30 keV energy range) using full Penn algorithm (FPA) from ELFs for elemental solids.

# Stopping Power calculation

:Relativistic DCS ( $< 0.5$  MeV)

$$\frac{d^2\sigma}{d\omega dq} = \frac{d^2\sigma_L}{d\omega dq} + \frac{d^2\sigma_T}{d\omega dq} \approx \frac{2}{\pi N v^2} \operatorname{Im} \left( \frac{-1}{\varepsilon(q, \omega)} \right) \frac{1}{q}$$

: Probability  $P(T, \omega)$  for energy loss per unit distance traveled by an electron with relativistic kinetic energy  $T$ .

$$p(T, \omega) = \frac{2}{\pi v^2} \int_{q_-}^{q_+} \frac{dq}{q} \operatorname{Im} \left[ \frac{-1}{\varepsilon(q, \omega)} \right] = \frac{(1 + T/c^2)^2}{1 + T/(2c^2)} \frac{1}{\pi T} \int_{q_-}^{q_+} \frac{dq}{q} \operatorname{Im} \left[ \frac{-1}{\varepsilon(q, \omega)} \right]$$

$$q_{\pm} = \sqrt{T(2 + T/c^2)} \pm \sqrt{(T - \omega)(2 + (T - \omega)/c^2)}$$

$$S(T) = \int_0^{\omega_{\max}} \omega p(T, \omega) d\omega$$

# Full Penn Algorithm for ELF calculation

The ELF in the FPA can be expressed as:

$$\text{Im} \left[ \frac{-1}{\varepsilon(q, \omega)} \right] = \int_0^\infty d\omega_p g(\omega_p) \text{Im} \left[ \frac{-1}{\varepsilon^L(q, \omega; \omega_p)} \right] \quad \leftarrow \text{Lindhard ELF}$$

$$g(\omega) = \frac{2}{\pi\omega} \text{Im} \left[ \frac{-1}{\varepsilon(\omega)} \right] \quad \leftarrow \text{Optical ELF (measured)}$$

$$\text{Im} \left[ \frac{-1}{\varepsilon^L(q, \omega; \omega_p)} \right] = \frac{\varepsilon_2^L}{(\varepsilon_1^L)^2 + (\varepsilon_2^L)^2}$$

$$\varepsilon_1^L(q, \omega; \omega_p) = 1 + \frac{1}{\pi k_F z^2} \left[ \frac{1}{2} + \frac{1}{8z} \left\{ F\left(z - \frac{x}{4z}\right) + F\left(z + \frac{x}{4z}\right) \right\} \right]$$

$$\varepsilon_2^L(q, \omega; \omega_p) = \frac{1}{8k_F z^3} \times \begin{cases} x & \text{for } 0 < x < 4z(1-z) \\ 1 - (z - (x/4z))^2 & \text{for } |4z(1-z)| < x < 4z(1+z), \\ 0 & \text{otherwise} \end{cases}$$

# Conditions and materials for SP calculations

Energy range for SP calculations: 10 eV to 30,000 eV

- calculated at equal intervals on a logarithmic energy scale corresponding to increases of 10 %.

- 41 elemental solids

Li, Be, diamond, graphite, glassy carbon, Na, Mg, Al, Si, K, Sc, Ti, V, Cr, Fe, Co, Ni, Cu, Ge, Y, Nb, Mo, Ru, Rh, Pd, Ag, In, Sn, Cs, Gd, Tb, Dy, Hf, Ta, W, Re, Os, Ir, Pt, Au, and Bi.

red: newer ELF data set (compared with previous calcs.)

## 2. Calculated results of SPs with FPA

- Single pole approximation (SPA) : [solid circles](#)
  - previous work (Surf. Interface Anal. 37 (2005) 978., J. Appl. Phys. 103 (2008) 063707. )
- Relativistic Bethe equation: [dashed lines](#)

$$S/\rho = \frac{784.58Z}{m_e v^2 A} \left[ \ln(T/I)^2 + \ln(1 + \tau/2) + G(\tau) \right]$$

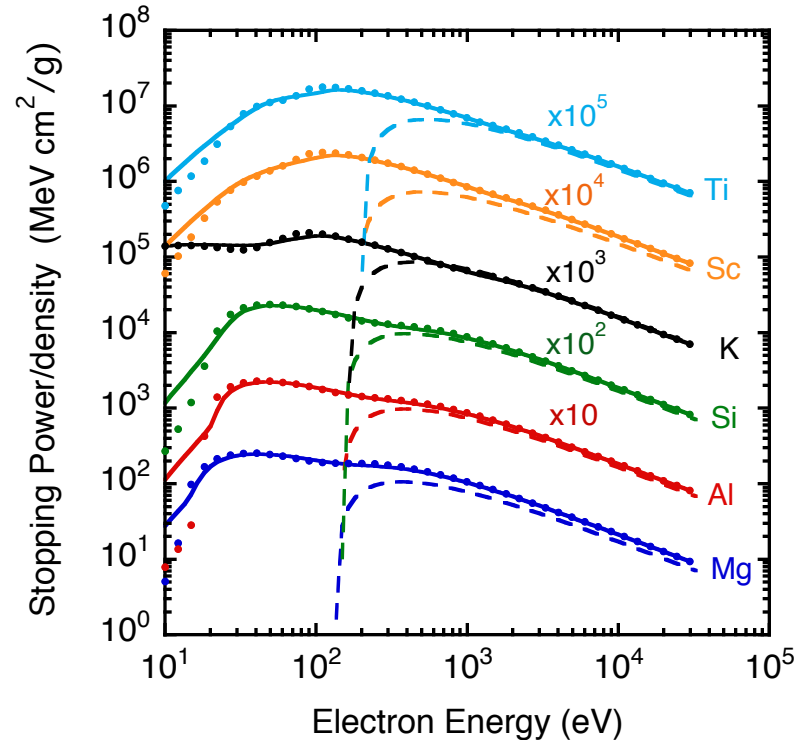
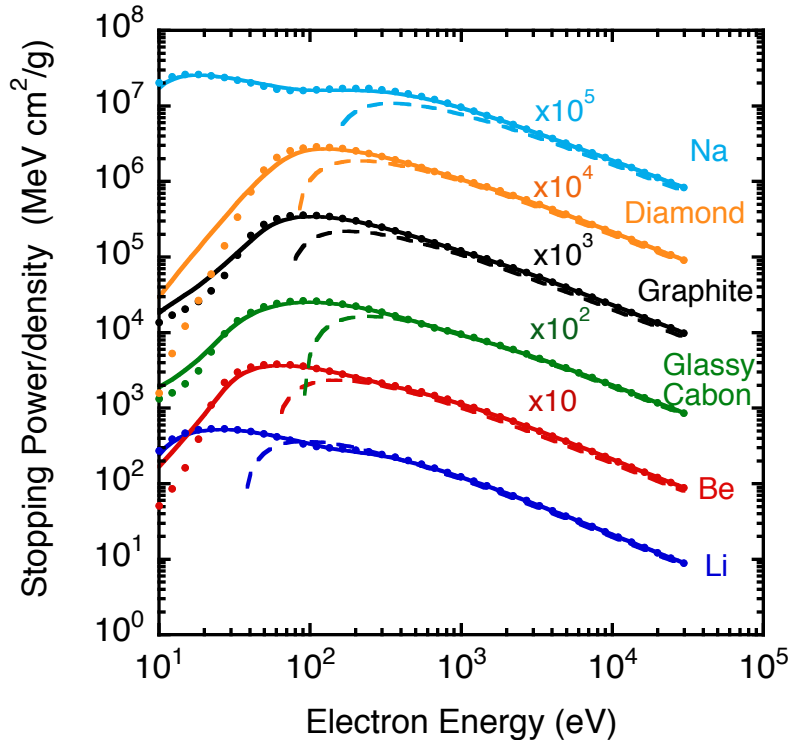
---

$$\tau = T/m_0c^2$$

$I$  : Mean excitation energy (MEE) , parameter

$T$  : electron relativistic energy ,  $Z$  : atomic number,  $\rho$ : density,  $A$ : atomic weight,

# Calculated SPs with FPA $z=3 - 22$

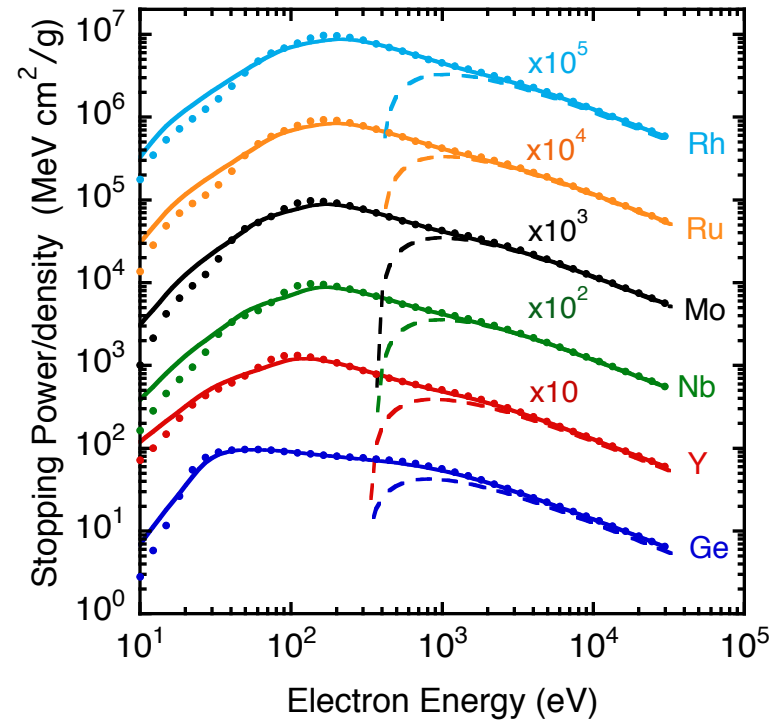
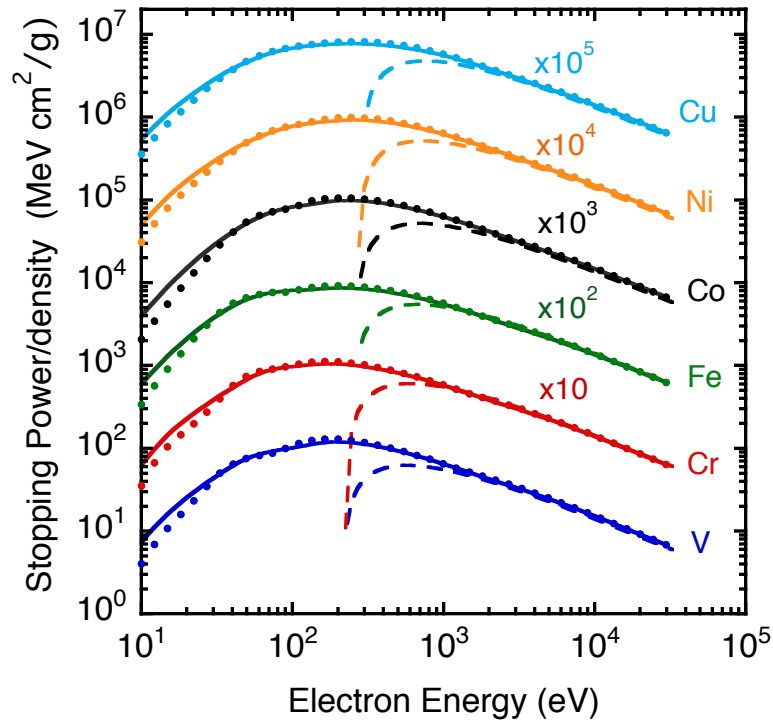


**Solid lines: SPs with FPA    Solid circles : SPs with SPA**  
**Dashed lines: relativistic Bethe equation**

*I* for Bethe equation: *ICRU report* (1984) and previous work for glassy carbon, graphite and diamond

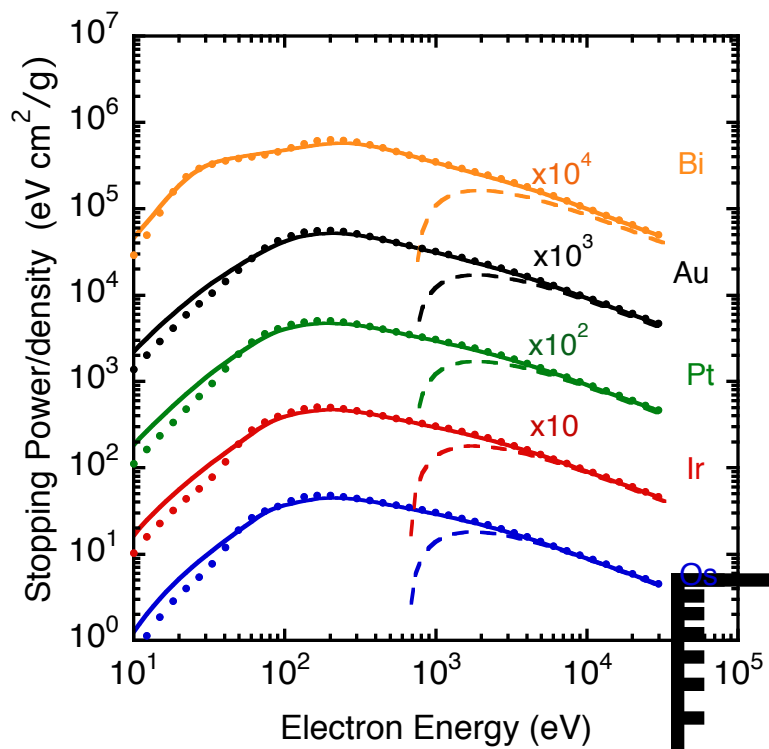
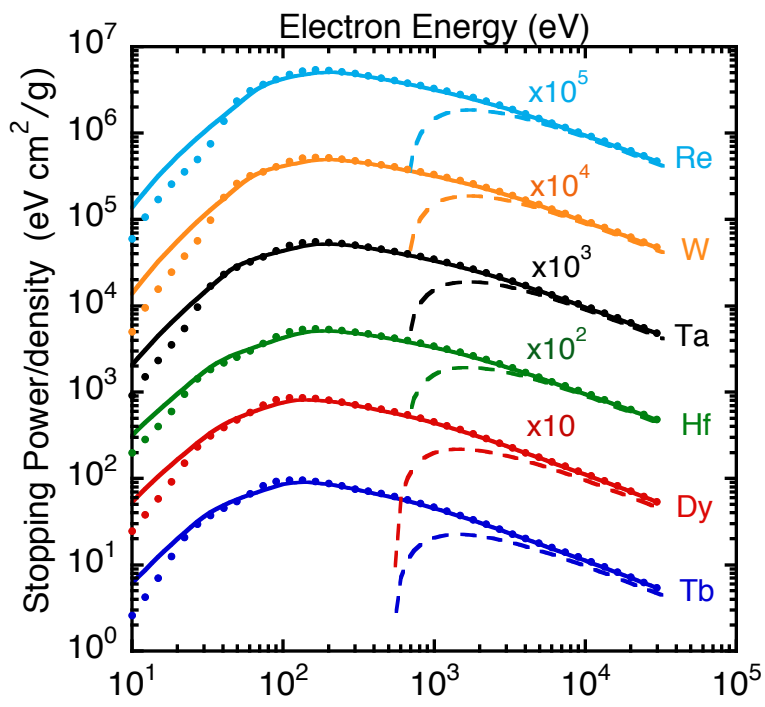
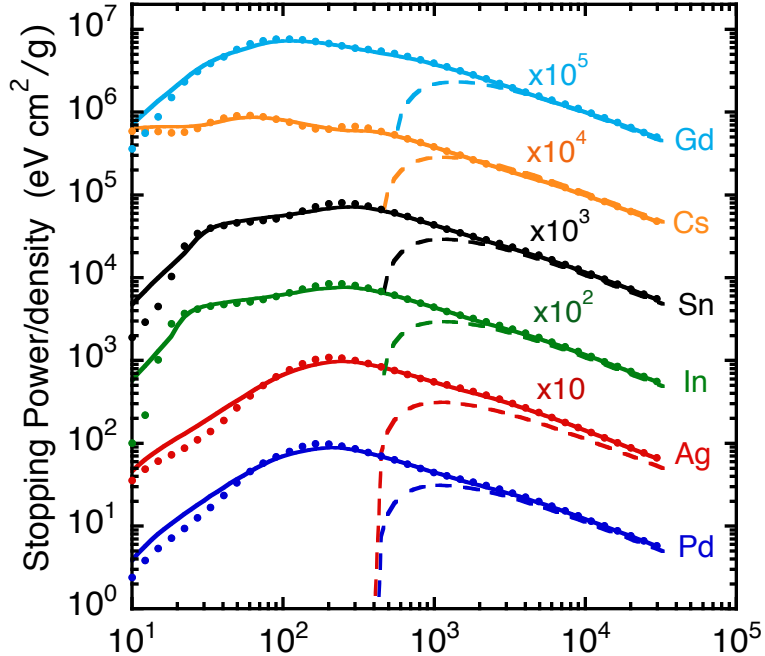
- multiple peaks and shoulders : valence electron and inner-shell excitation

# Calculated SPs with FPA $z=23 - 45$

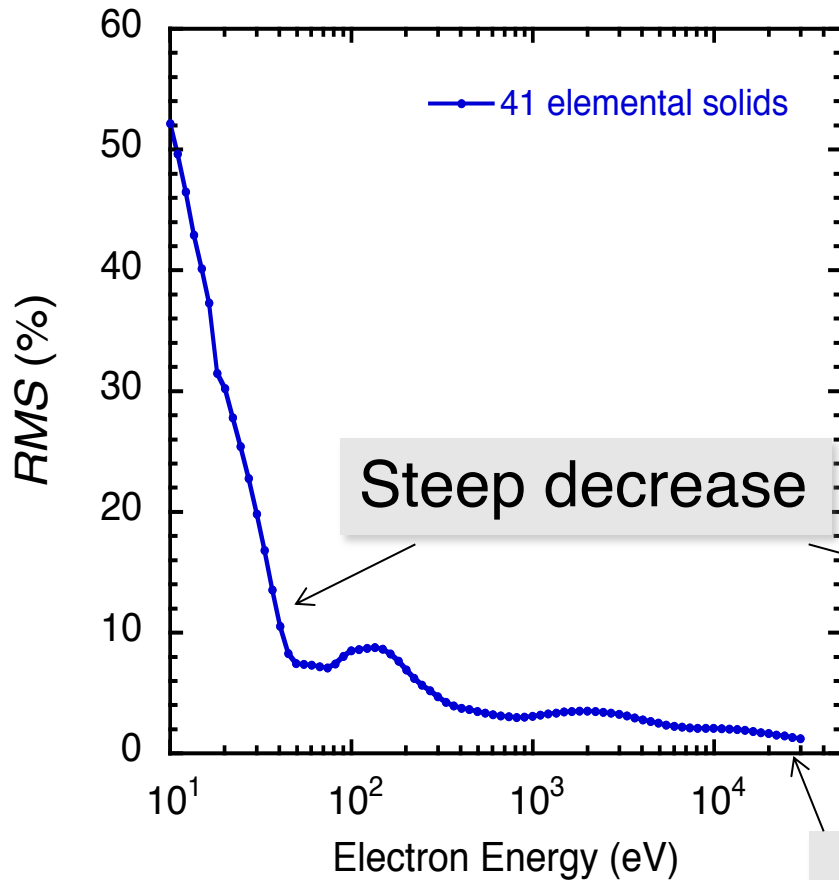


**Solid lines: SPs with FPA    Solid circles : SPs with SPA**  
**Dashed lines: relativistic Bethe equation**

# Calculated SPs with FPA z= 46 - 83



# Comparison of stopping powers from the FPA and SPA



- comparisons of RMS differences between SPs calculated from the FPA and SPA for 41 solids. Relative percentage RMS differences, RMS, were calculated from

$$RMS = 100 \times \left[ \sum_{i=1}^{41} \left( \frac{S_{SPA}(T)_i - S_{FPA}(T)_i}{S_{FPA}(T)_i} \right)^2 / 41 \right]^{0.5}$$

- contributions of single-electron excitations to the SP that are neglected in the SPA

- RMS generally decreases with increasing energy, reaching 1 % at 30 keV

# Influence of electron exchange on SPs

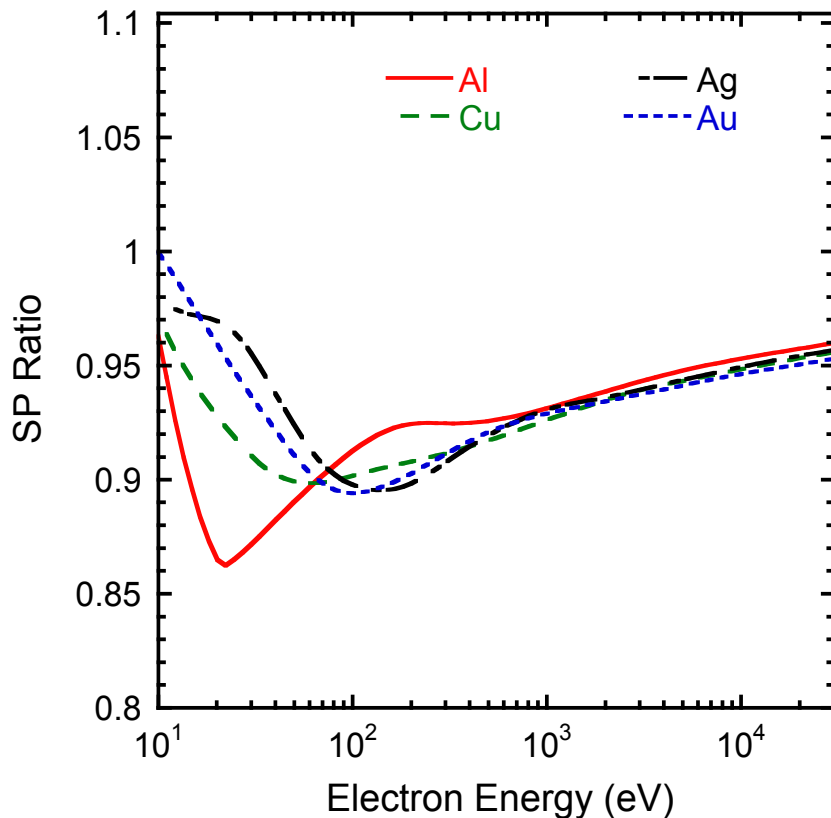
- important to know the effect of exchange between projectile and target electrons on SP calculations with the FPA.
- no consensus on how to incorporate exchange effects within the dielectric formalism
- estimate the influence of electron exchange on SPs using the Born-Ochkur exchange correction.

The non-relativistic DCS with the Born-Ochkur correction can be written as

$$\frac{d^2\sigma}{dq d\omega} = \left( 1 - \frac{q^2}{2E} + \left( \frac{q^2}{2E} \right)^2 \right) \frac{1}{\pi N E} \operatorname{Im} \left[ \frac{-1}{\varepsilon(q, \omega)} \right] \frac{1}{q}$$

-calculated SPs of **Al, Cu, Ag, and Au** with and without the exchange correction and compared them.

# Influence of electron exchange on SPs



SP ratio = SP **with** exchange  
/ SP **without** exchange

- SPs with the exchange correction are smaller than those without the exchange correction for these four solids and energies between 10 eV and 30 000 eV

- Above 100 eV, SPs with exchange correction are smaller than SPs without exchange correction by less than about 10%

- The influence of electron exchange on calculated SPs is almost the same as that found in IMFP calculations for electron energies between 50 eV and 100 eV. (CJP & AJ)

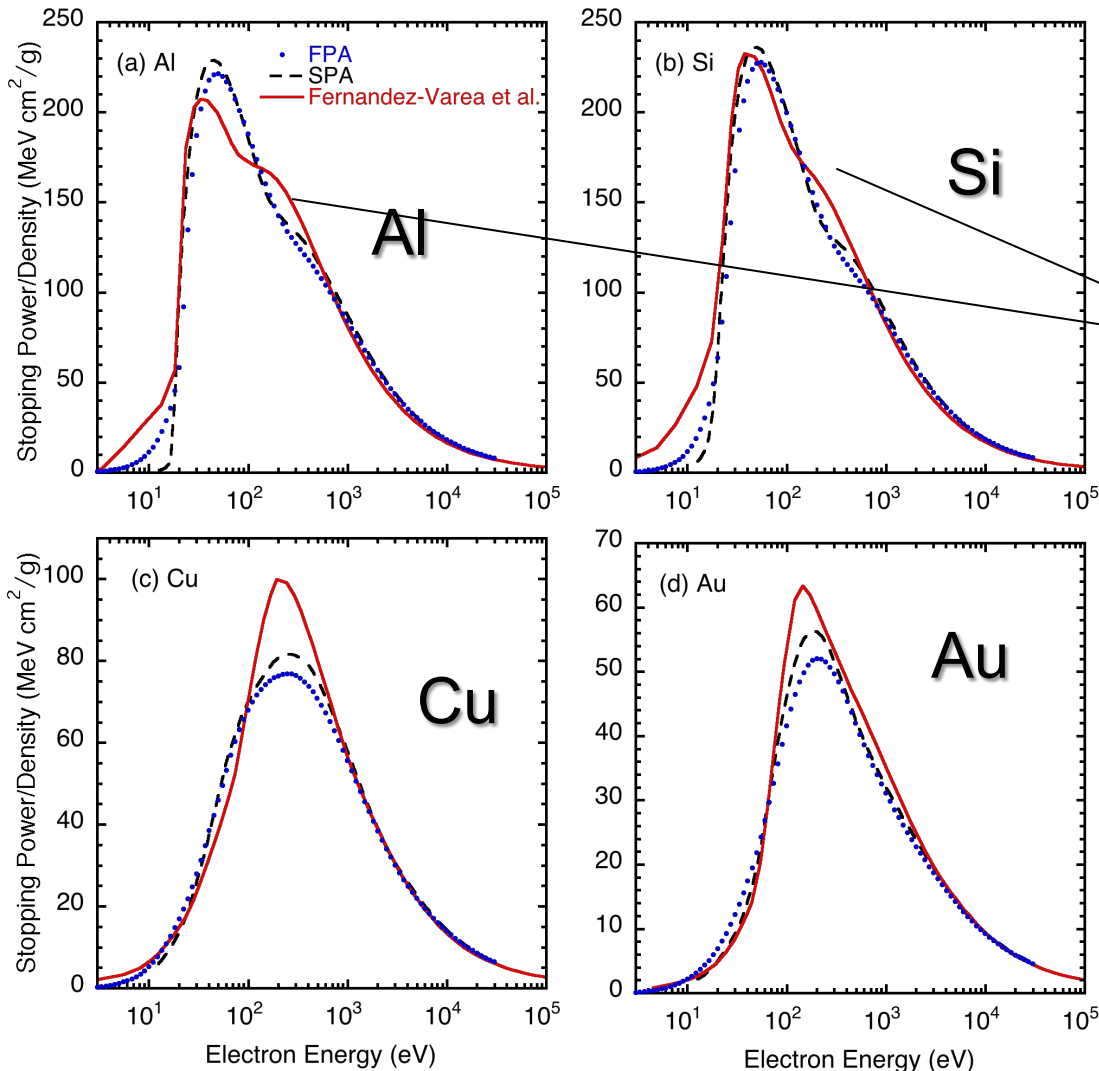
- Born-Ochkur corr. is essentially a high-energy approximation. It is then not clear whether this approximation is useful for evaluating the exchange correction for energies less than 100 eV.

### 3. Comparisons with calculated SPs (1)

[Fernandez-Varea \*et al.\*](#) calculated SPs for Al, Si, Cu, and Au for electron energies between 10 eV and 100 MeV.

- based on a so-called “N-oscillator” model in which different dispersion relations were applied for valence-electron excitations and inner-shell excitations.
- included a correction for electron exchange to cross sections for inner-shell excitations .

# (1) Comparisons of SPs : Fernandez-Varea et al.



- For energies over 1000 eV, the SPs of Fernandez-Varea *et al.* for Al, Si, Cu, and Au are in excellent agreement with our values from the FPA.

- These shape differences might be associated with the “switch energies” of 73 eV and 99 eV for Al and Si, respectively, used by Fernandez-Varea *et al.* to represent the demarcation between their models for valence-electron and inner-shell excitations.

- For Cu and Au, the switch energies are 74 eV and 54 eV, respectively, but there are no obvious changes of slope in the SP-energy curve. This might be due to the structure-less region of their ELFs.

### 3. Comparisons with calculated SPs (2)

**Abril et al.** proposed an algorithm for IMFP and SP calculations based largely on a Mermin-model dielectric function for the ELF (**Mermin-ELF model**). The Mermin function is an improvement over the Lindhard dielectric function used in Penn algorithm in that it accounts for the finite lifetimes of the various excitations

- **Mermin-ELF model** q=0 :

$$\text{Im} \left[ \frac{-1}{\varepsilon_M(q=0, \omega)} \right]_{outer} = \sum_i A_i \text{Im} \left[ \frac{-1}{\varepsilon_D(q=0, \omega; \omega_{p,i}, \gamma_i)} \right]$$

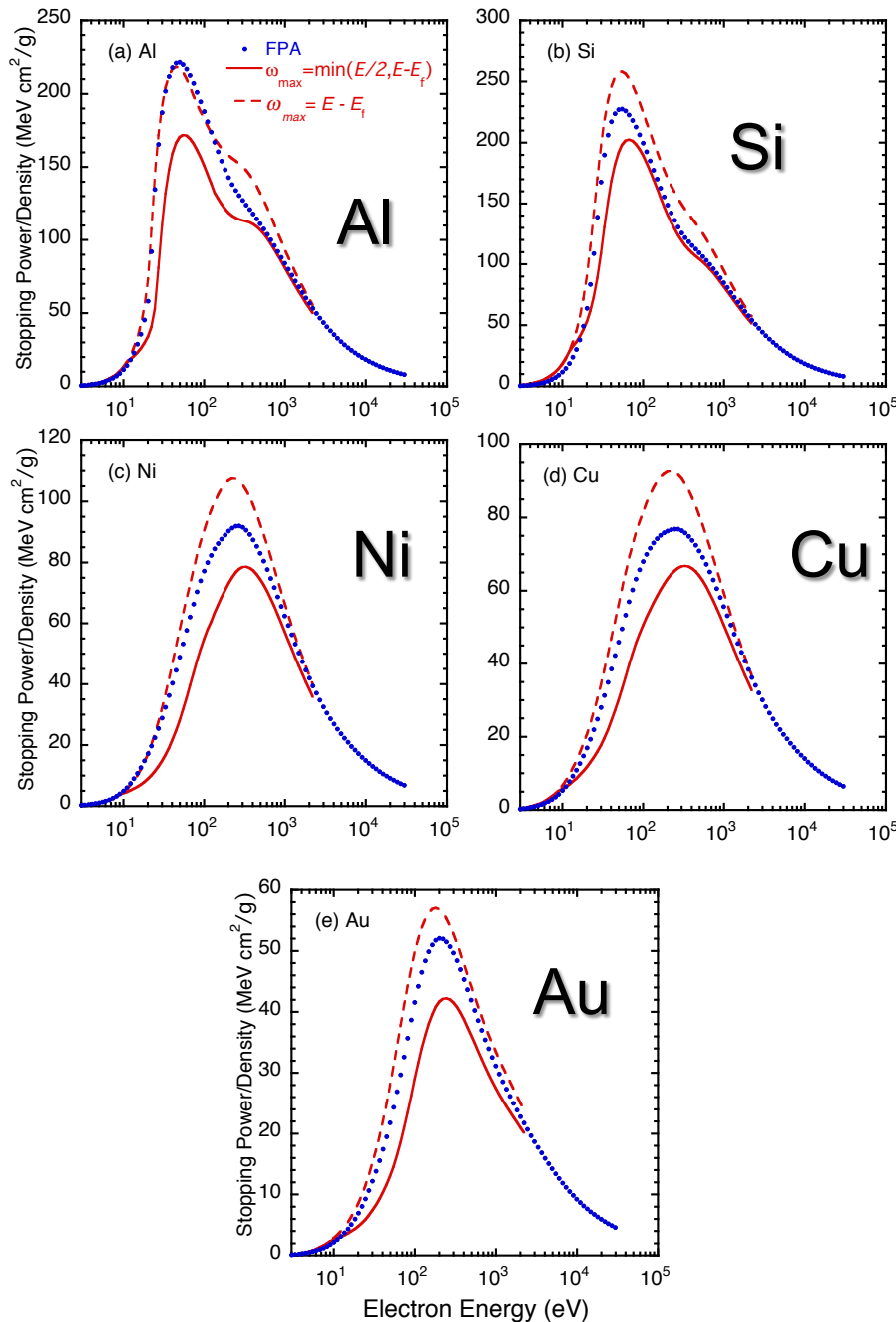
Drude type ELF

parameters: relative weight, position, and width

- **q dependence** (q>0) 
$$\varepsilon_M(q, \omega) = 1 + \frac{1 + i\gamma / \omega}{[\varepsilon_L(q, \omega + i\gamma) - 1]^{-1} + (i\gamma / \omega)[\varepsilon_L(q, 0) - 1]^{-1}}$$

- We have calculated SPs for Al, Si, Ni, Cu, and Au with the **Mermin-ELF model** using the parameters for outer-electron excitations given in Table of their reference.

## (2) Comparisons of SPs : Mermin model ELF



$$S(T) = \int_0^{\omega_{\max}} \omega p(T, \omega) d\omega$$

Solid lines:

$$\omega_{\max} = T/2 \quad T > 2E_f$$

Dashed lines:

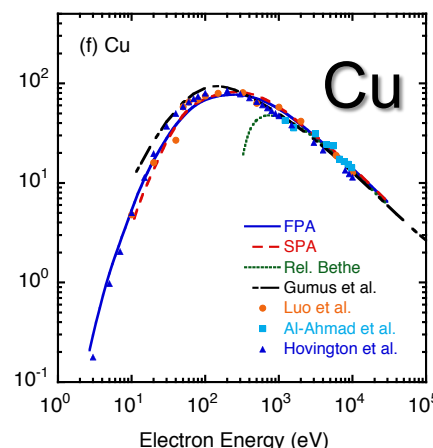
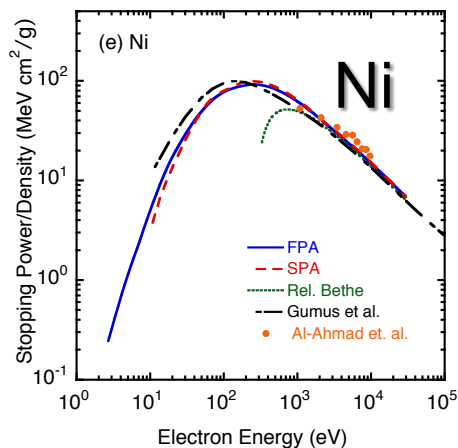
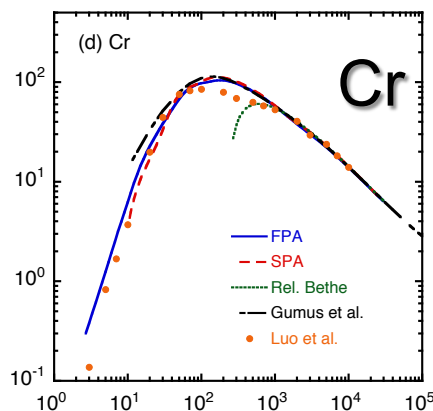
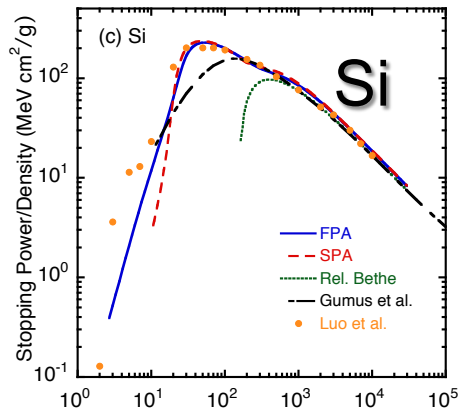
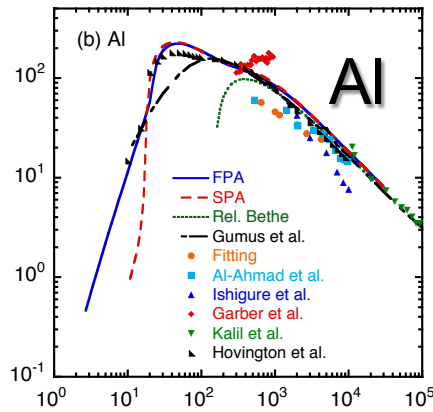
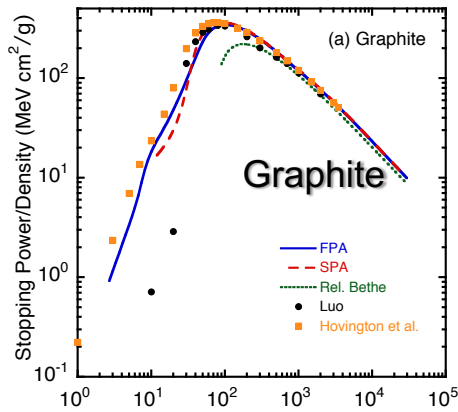
$$\omega_{\max} = T - E_f$$

- choice of the upper limit is more significant in SP calculations than in IMFP calculations because of the greater relative contributions of possible large-energy-loss excitations to the SP than to the IMFP.

## 4. Comparisons with experimental SPs

- We compared calculated SPs from the FPA for graphite, Al, Si, Cr, Ni, Cu, Ge, Pd, Ag, Pt, and Au with experimental SP data that were mostly obtained from Joy's database
- The experimental SPs can be classified into two groups.
- experimental SPs for energies less than 1 keV : These SPs are based on measurements of transmission electron energy-loss spectra of 100 keV or 200 keV electrons transmitted through thin specimen films.
- The other group of measured SPs was obtained from calorimetric methods for Al, Ni, Cu, Ag, and Au, from a novel thin-film

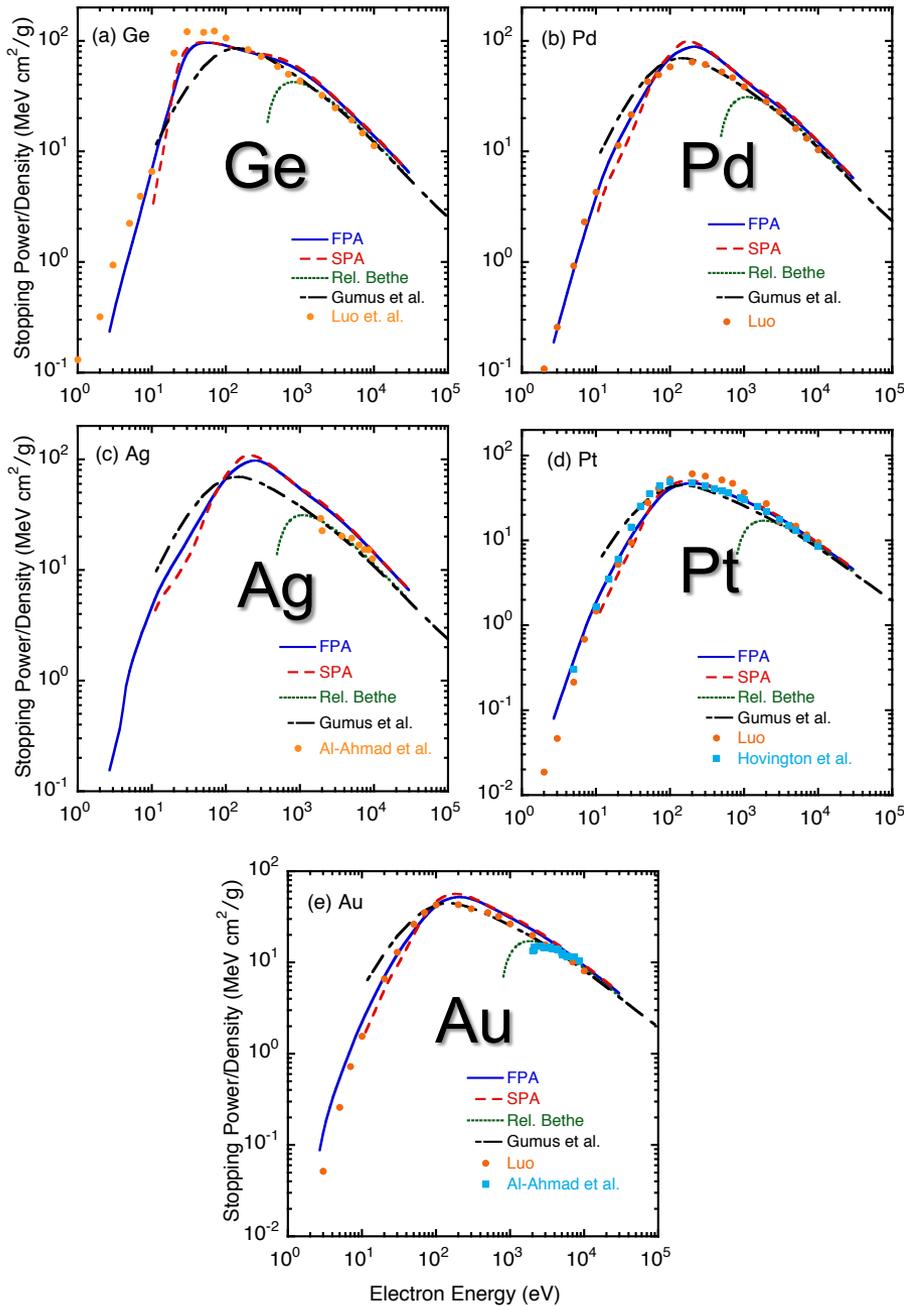
# (1) Comparisons of SPs : experimental SPs



- generally good agreement between our SPs from the FPA and the Joy SPs for energies larger than about 10 eV.

- In Cu and Cr (< 100 eV)  
- The excellent agreement at energies near 10 eV is very likely fortuitous because our SP calculations with the FPA ignored the effects of electron exchange and correlation that must be important at such low energies.

## (2) Comparisons of SPs : experimental SPs



- We also see a generally excellent agreement between our SPs from the FPA and the experimental SPs for energies larger than about 10 eV.

Solid line : SP with FPA  
 Dashed line: SP with SPA  
 Dotted line : rel. Bethe eq.  
 Mark : experimental SP  
 Long-short dashed line: mod. Bethe-Bloch eq. ( with effective atomic electron number and MEE)

# 5. Summary

- We reported electron SPs for 41 elemental solids over the 10 eV to 30 keV energy range. These SPs were calculated from ELF data determined from experimental optical data with the full Penn algorithm (FPA).
- We made comparisons of RMS differences between SPs calculated from the FPA and SPA using the same ELF data sets. For energies above 50 eV, the RMS relative differences were less than 10 % and generally decreased with increasing energy, reaching 1 % at 30 keV.
- We compared our calculated SPs with results from other calculations. (SPs by Fernandez-Varea et al., Abril et al. ) We see reasonable agreements over several keV region, but large differences under 1keV that are due to calculation model.

## 5. Summary continue

- We found generally excellent agreement between experimental SPs and our SPs from the FPA for energies larger than about 10 eV, although there were small but systematic differences for some solids between 10 eV and 100 eV.